PERGAMON

International Journal of Solids and Structures 39 (2002) 3023–3037

INTERNATIONAL JOURNAL OF SOLIDS and STRUCTURES

www.elsevier.com/locate/ijsolstr

Axi-symmetric wave propagation in a cylinder coated with a piezoelectric layer

Q. Wang *

Department of Civil Engineering, National University of Singapore, 10 Kent Ridge Crescent, Singapore 119260, Singapore

Received 27 March 2001; received in revised form 19 February 2002

Abstract

This paper presents the wave propagation in a cylinder coated with a thin piezoelectric layer. The piezoelectric coupling effects are fully modeled in the mechanics model for this piezoelectric coupled cylindrical shell with bending resistance. The decoupled torsional wave velocity and the dispersion curves for the two- mode shell model are obtained theoretically. The cut-off frequency and phase velocities at limit wave number are also derived. The numerical simulations are conducted to present the results of wave propagation in this cylindrical shell and as well as to compare the results by the current bending theory and the membrane shell theory. From the comparisons, the results display obvious deference of wave propagations in terms of dispersion characteristics by different shell theories when thicker piezoelectric layer are used and when higher wave number is considered. The results of this paper can serve as a reference for future study on wave propagation in coupled structures as well as in the design of smart structures incorporating piezoelectric materials.

Keywords: Dispersive curves; Piezoelectric coupled shell; Shells with bending resistance; Cut-off frequency; Torsional phase velocity

1. Introduction

The researches on wave propagation and vibration in pure piezoelectric structures have been received considerable attention previously as exhibited by the work of Mindlin (1952), Tiersten (1963) and Bluestein (1969). Research on its application for time delay devices has been investigated (Viktorov, 1967, 1981; Curtis and Redwood, 1973; Sun and Cheng, 1974). Wave propagation and vibration in piezoelectric coupled structures have been studied as well recently (see the work by Minagawa (1995) and Ding et al. (1997)). One of the important potential applications of wave propagation in piezoelectric structures is about the using of interdigital transducer (IDT). IDT was first used to excite the surface wave devices in radar communication equipment as filters and delay lines (Varadan and Varadan, 2000), and some consumer areas such as pagers, mobile phone, and sensors (Morgan, 1998; Campbell, 1998; White, 1998).

* Tel.: +65-779-1635; fax: +65-874-4683.
E-mail address: cvewangq@nus.edu.sg (Q. Wang).

0020-7683/02/$ - see front matter
PII: S0020-7683(02)00233-0

Its important application in separating, amplifying, and storing signals and in other signal processing applications in acoustic electronics were also paid attentions to (Auld, 1973a,b; Parton and Kudryavtser, 1988).

An important application of the piezoelectric materials is the health monitoring of structures by using IDT. This application requires a piezoelectric layer surface bonded on the structures to be health monitored, and the IDT is used to excite a wave propagating in the piezoelectric coupled structure to study the wave signal for the purpose of damage detection of the host structure. Some methods and experimental works on the rapid monitoring of structures using IDT to excite Lamb wave have been attempted (Badcock and Birt, 2000; Monkhouse et al., 2000) in some plate-like structures. The use of IDT in the health monitoring of a cylindrical shell structure requires the model of wave propagation in this piezoelectric coupled shell structure. To the author's knowledge, there are few works on the above research. Wave propagation in an axi-symmetric cylindrical shell has been studied by Wang (2001) by membrane shell theory. As higher wave numbers are usually of interest in the wave propagation problems, higher order theories for shell structures are necessary in the modelling of shell structures.

The wave propagation in a shell structure had been studied for decades. The simplest membrane shell model was put forth by Love (1944), in which the transverse forces, bending and twisting moments are negligible. Such model is suitable for thin shell structures in which only normal and shear forces acting in the mid-surface of the shell are considered. Although it is a low-order shell model, it is easy to present the essential features of the shell, and what is more, it provides basic model for higher-order shell model in which shear and twisting effects are considered. Some slight modified theories based on this simply model was presented by Flüggey (1934), Vlasov (1949), Donnel (1933), Sanders (1959). Mersky and Herrmann (1958) included shear effects in both the axial and circumferential direction and rotary-inertia effects in the study of axially symmetric waves in a cylindrical shell. Lin and Morgan (1956) developed the equations for axially symmetric motions including shear effects and rotary-inertia effects. Cooper and Naghdi (1957) presented a theory including shear effects and rotary-inertia for non-axially symmetric motion of shell structures. A comparison study of wave propagation in a cylindrical shell by different shell theories by Greenspon (1960) shows obvious discrepancies in studying dispersion curves of the shell structure by different theories, especially at higher wave numbers.

The objective of this paper is to present the results of axi-symmetric wave motions in piezoelectric coupled cylindrical shells with bending resistance by shell bending model under the inherent shear-rigidity assumption. The dispersion curves for different ratios of the thickness of the piezoelectric layer to the thickness of the host shell structure, as well as different core materials of the cylindrical shell are obtained by the model. In addition, the phase velocity at limit wave number and cut-off frequency are also presented. Comparison of the wave propagation in this piezoelectric shell by the bending theory in the paper and the membrane shell theory Wang (2001) are also conducted to show the validity of the different shell theories in view of wave propagation problems in the piezoelectric coupled cylindrical shells.

2. Mechanics model of the piezoelectric coupled cylindrical shell with bending resistance

A thin shell surface bonded by a piezoelectric layer is shown in Fig. 1(a). This shell with bending resistance is under Love's shear-rigidity assumption. This assumption indicates that a certain plane perpendicular to the mid-plane will still remain perpendicular to the mid-plane after deformation. The coordinate is set to indicate the coordinates x for the direction along the shell, θ for the direction of polar angel, and r for the radial direction. The stress analysis on an infinitesimal element of the shell structure is shown in Fig. 1(b). The governing equations of motion in the longitudinal, tangential, and radial directions are, respectively,

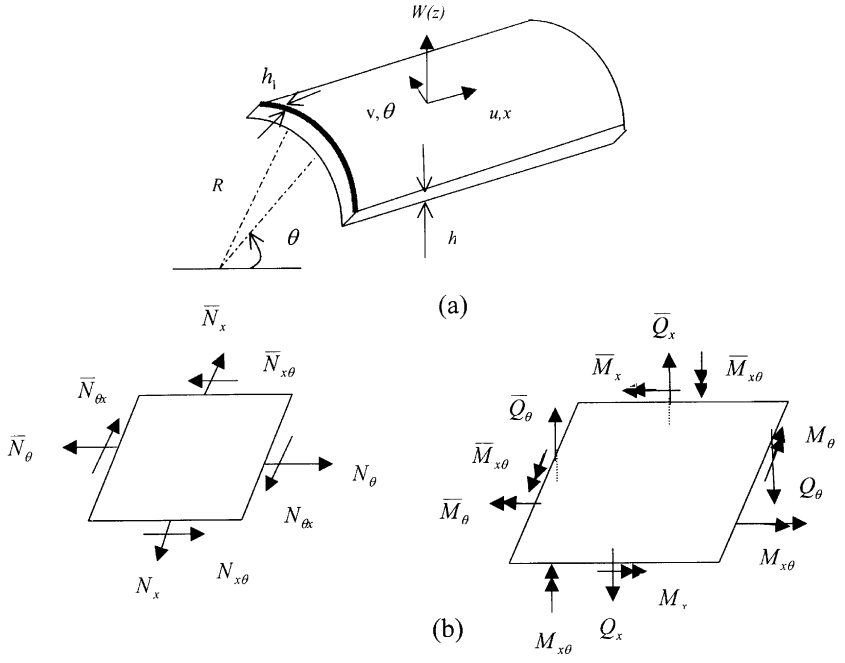

$$\bar{N}_x = N_x + \frac{\partial N_x}{\partial x}dx \qquad \bar{N}_\theta = N_\theta + \frac{\partial N_\theta}{\partial \theta}d\theta \qquad \bar{N}_{x\theta} = N_{x\theta} + \frac{\partial N_{x\theta}}{\partial x}dx$$

$$\bar{M}_x = M_x + \frac{\partial M_x}{\partial x}dx \qquad \bar{M}_\theta = M_\theta + \frac{\partial M_\theta}{\partial \theta}d\theta \qquad \bar{M}_{x\theta} = M_{x\theta} + \frac{\partial M_{x\theta}}{\partial x}dx$$

$$\bar{Q}_x = Q_x + \frac{\partial Q_x}{\partial x}dx$$

Fig. 1. A piezoelectric thin membrane shell (a) layout, (b) the stress analysis at an infinitesimal element.

$$\frac{\partial N_x}{\partial x} + \frac{\partial N_{\theta x}}{R\partial \theta} = \left(\rho h + \rho' h_1\right)\frac{\partial^2 u}{\partial t^2} \tag{1}$$

$$\frac{\partial N_\theta}{R\partial \theta} + \frac{\partial N_{x\theta}}{\partial x} - \frac{Q_\theta}{R} = \left(\rho h + \rho' h_1\right)\frac{\partial^2 v}{\partial t^2} \tag{2}$$

$$\frac{\partial Q_x}{\partial x} + \frac{\partial Q_\theta}{R\partial \theta} - \frac{N_\theta}{R} = \left(\rho h + \rho' h_1\right)\frac{\partial^2 w}{\partial t^2} \tag{3}$$

$$\frac{\partial M_x}{\partial x} + \frac{\partial M_{x\theta}}{R\partial \theta} - Q_x = 0 \tag{4}$$

$$\frac{\partial M_{x\theta}}{\partial x} + \frac{\partial M_\theta}{R\partial \theta} - Q_\theta = 0 \tag{5}$$

where u, v, and w are the longitudinal, transverse, and radial displacement of the section; R is the radius of the shell; h and h_1 are thickness of the shell and the piezoelectric layer; and ρ and ρ' are mass densities of the

shell and the layer; N_x, $N_{\theta x}$, $N_{x\theta}$, and N_θ are membrane stresses; M_x, $M_{\theta x}$, and M_θ are stress couples; Q_x and Q_θ are normal shear stresses shown in Fig. 1(b).

Substituting Eqs. (4) and (5) into Eqs. (2) and (3) yields,

$$\frac{\partial N_\theta}{R\partial\theta}+\frac{\partial N_{x\theta}}{\partial x}-\frac{1}{R}\left(\frac{\partial M_{x\theta}}{\partial x}+\frac{\partial M_\theta}{R\partial\theta}\right)=\left(\rho h+\rho' h_1\right)\frac{\partial^2 v}{\partial t^2} \tag{6}$$

$$\frac{\partial^2 M_x}{\partial x^2}+\frac{2\partial^2 M_{x\theta}}{R\partial x\partial\theta}+\frac{\partial^2 M_\theta}{R^2\partial\theta^2}-\frac{N_\theta}{R}=\left(\rho h+\rho' h_1\right)\frac{\partial^2 w}{\partial t^2} \tag{7}$$

Thus, the governing equation for the wave propagation in this cylindrical shell by the bending theory is expressed by Eqs. (1), (6), and (7).

The membrane stresses and bending stresses are obtained by integrating the stresses across the thickness of the shell as follows:

$$N_x=\int_{-\frac{h}{2}}^{\frac{h}{2}}\sigma_x^1\,\mathrm{d}z+\int_{\frac{h}{2}}^{\frac{h}{2}+h_1}\sigma_x^2\,\mathrm{d}z \tag{8}$$

$$N_\theta=\int_{-\frac{h}{2}}^{\frac{h}{2}}\sigma_\theta^1\,\mathrm{d}z+\int_{\frac{h}{2}}^{\frac{h}{2}+h_1}\sigma_\theta^2\,\mathrm{d}z \tag{9}$$

$$N_{\theta x}=N_{x\theta}=\int_{-\frac{h}{2}}^{\frac{h}{2}}\tau_{x\theta}^1\,\mathrm{d}z+\int_{\frac{h}{2}}^{\frac{h}{2}+h_1}\tau_{x\theta}^2\,\mathrm{d}z \tag{10}$$

$$M_x=\int_{-\frac{h}{2}}^{\frac{h}{2}}z\sigma_x^1\,\mathrm{d}z+\int_{\frac{h}{2}}^{\frac{h}{2}+h_1}z\sigma_x^2\,\mathrm{d}z \tag{11}$$

$$M_\theta=\int_{-\frac{h}{2}}^{\frac{h}{2}}z\sigma_\theta^1\,\mathrm{d}z+\int_{\frac{h}{2}}^{\frac{h}{2}+h_1}z\sigma_\theta^2\,\mathrm{d}z \tag{12}$$

$$M_{x\theta}=\int_{-\frac{h}{2}}^{\frac{h}{2}}z\tau_{x\theta}^1\,\mathrm{d}z+\int_{\frac{h}{2}}^{\frac{h}{2}+h_1}z\tau_{x\theta}^2\,\mathrm{d}z \tag{13}$$

where σ_x, σ_θ, and $\tau_{x\theta}$ are the normal and shear stresses distributed in the host shell and the piezoelectric layer, and the superscripts 1 and 2 represent the variables in the host shell and the piezoelectric layer respectively.

The poling direction of the piezoelectric material is assumed to be in the axial x-direction of shell, which also means the x-direction is the axis of symmetry for the piezoelectric layer. The relationship of the strains ε_x, ε_θ, and $\gamma_{x\theta}$, and stresses σ_x, σ_θ, and $\tau_{x\theta}$ in the shell and piezoelectric layer may be obtained accordingly as

$$\sigma_x^1=\frac{E}{1-v^2}\left(\varepsilon_x+v\varepsilon_\theta\right) \tag{14}$$

$$\sigma_\theta^1=\frac{E}{1-v^2}\left(\varepsilon_\theta+v\varepsilon_x\right) \tag{15}$$

$$\tau_{x\theta}^1=\gamma_{x\theta}\frac{E}{2(1+v)} \tag{16}$$

$$\sigma_x^2 = c_{33\mathrm{p}}\varepsilon_x + c_{13\mathrm{p}}\varepsilon_\theta - e_{33\mathrm{p}}E_x = c_{33\mathrm{p}}\varepsilon_x + c_{13\mathrm{p}}\varepsilon_\theta + e_{33\mathrm{p}}\frac{\partial\varphi}{\partial x} \tag{17}$$

$$\sigma_\theta^2 = c_{11\mathrm{p}}\varepsilon_\theta + c_{13\mathrm{p}}\varepsilon_x - e_{31\mathrm{p}}E_x = c_{11\mathrm{p}}\varepsilon_\theta + c_{13\mathrm{p}}\varepsilon_x + e_{31\mathrm{p}}\frac{\partial\varphi}{\partial x} \tag{18}$$

$$\tau_{x\theta}^2 = c_{44\mathrm{p}}\gamma_{x\theta} - e_{15\mathrm{p}}E_\theta = c_{44\mathrm{p}}\gamma_{x\theta} + e_{15\mathrm{p}}\frac{\partial\varphi}{R\,\partial\theta} \tag{19}$$

where φ and $E_x = (\partial\varphi/\partial x)$ are variables of the electric potential and the electric field distributed in the piezoelectric layer; E and v are the Young's modulus and Poisson ratio of host shell material; $c_{33\mathrm{p}} = c_{33} - (c_{13}^2/c_{11})$, $c_{13\mathrm{p}} = c_{13} - (c_{12}c_{13}/c_{11})$, $c_{11\mathrm{p}} = c_{11} - (c_{12}^2/c_{11})$, $c_{44\mathrm{p}} = c_{44}$ are effective elastic module of the piezoelectric layer for plane stress problem; $e_{31\mathrm{p}} = e_{31} - (c_{12}/c_{11})e_{31}$, $e_{15\mathrm{p}} = e_{15}$, $e_{33\mathrm{p}} = e_{33} - (c_{13}/c_{11})e_{31}$ are effective piezoelectric constants of the piezoelectric layer for plane stress problem.

Under Love's assumption in shell theory, the corresponding strains in the current coordinate system are expressed as (Love, 1944)

$$\varepsilon_x = \frac{\partial u}{\partial x} - z\frac{\partial^2 w}{\partial x^2} \tag{20}$$

$$\varepsilon_\theta = \frac{1}{R}\left(w + \frac{\partial v}{\partial\theta}\right) - z\frac{\partial^2 w}{R^2\,\partial\theta^2} \tag{21}$$

$$\gamma_{x\theta} = \frac{\partial v}{\partial x} + \frac{\partial u}{R\,\partial\theta} - 2z\frac{\partial^2 w}{R\,\partial x\,\partial\theta} \tag{22}$$

It is obvious from the above proposed kinematics field that, in the current study of wave propagation in this cylindrical shell, the piezoelectric layer is assumed to be very thin. Thus the middle session of the host cylinder can still be assumed to remain un-deformed even after the layer of the piezoelectric material is coated.

Substituting Eqs. (20)–(22) into Eqs. (8)–(13) gives,

$$N_x = A_1\frac{\partial u}{\partial x} + \frac{A_2}{R}\left(w + \frac{\partial v}{\partial\theta}\right) + A_3\frac{\partial^2 w}{\partial x^2} + A_4\frac{\partial^2 w}{R^2\,\partial\theta^2} + A_5\frac{\partial\varphi}{\partial x} \tag{23}$$

$$N_\theta = \frac{B_1}{R}\left(w + \frac{\partial v}{\partial\theta}\right) + B_2\frac{\partial u}{\partial x} + B_3\frac{\partial^2 w}{R^2\,\partial\theta^2} + B_4\frac{\partial^2 w}{\partial x^2} + B_5\frac{\partial\varphi}{\partial x} \tag{24}$$

$$N_{x\theta} = C_1\left(\frac{\partial v}{\partial x} + \frac{\partial u}{R\,\partial\theta}\right) + C_2\frac{\partial^2 w}{R\,\partial x\,\partial\theta} + C_3\frac{\partial\varphi}{R\,\partial\theta} \tag{25}$$

$$M_x = D_1\frac{\partial^2 w}{\partial x^2} + D_2\frac{\partial^2 w}{R^2\,\partial\theta^2} + D_3\frac{\partial u}{\partial x} + \frac{D_4}{R}\left(w + \frac{\partial v}{\partial\theta}\right) + D_5\frac{\partial\varphi}{\partial x} \tag{26}$$

$$M_\theta = E_1\frac{\partial^2 w}{R^2\,\partial\theta^2} + E_2\frac{\partial^2 w}{\partial x^2} + \frac{E_3}{R}\left(w + \frac{\partial v}{\partial\theta}\right) + E_4\frac{\partial u}{\partial x} + E_5\frac{\partial\varphi}{\partial x} \tag{27}$$

$$M_{x\theta} = F_1\frac{\partial^2 w}{R\,\partial x\,\partial\theta} + F_2\left(\frac{\partial v}{\partial x} + \frac{\partial u}{R\,\partial\theta}\right) + F_3\frac{\partial\varphi}{R\,\partial\theta} \tag{28}$$

where the expressions of A_i $(i=1,\ldots,6)$, B_i $(i=1,\ldots,6)$, C_i $(i=1,\ldots,3)$, D_i $(i=1,\ldots,5)$, E_i $(i=1,\ldots,5)$, and F_i $(i=1,\ldots,3)$ are shown in Appendix A.

Then the governing Eqs. (1), (6) and (7) become,

$$A_1\frac{\partial^2 u}{\partial x^2}+\frac{A_2}{R}\left(\frac{\partial w}{\partial x}+\frac{\partial^2 v}{\partial x\,\partial\theta}\right)+A_3\frac{\partial^3 w}{\partial x^3}+A_4\frac{\partial^3 w}{R^2\,\partial x\,\partial\theta^2}+A_5\frac{\partial^2\varphi}{\partial x^2}\,C_1\left(\frac{\partial^2 v}{R\,\partial\theta\,\partial x}+\frac{\partial^2 u}{R^2\,\partial\theta^2}\right)+C_2\frac{\partial^3 w}{R^2\,\partial x\,\partial\theta^2}+C_3\frac{\partial^2\varphi}{R^2\,\partial\theta^2}=\left(\rho h+\rho' h_1\right)\frac{\partial^2 u}{\partial t^2} \tag{29}$$

$$\frac{B_1}{R^2}\left(\frac{\partial w}{\partial\theta}+\frac{\partial^2 v}{\partial\theta^2}\right)+\frac{B_2}{R}\frac{\partial^2 u}{\partial x\,\partial\theta}+\frac{B_3}{R^3}\frac{\partial^3 w}{\partial\theta^3}+\frac{B_4}{R}\frac{\partial^3 w}{\partial\theta\,\partial x^2}+\frac{B_5}{R}\frac{\partial^2\varphi}{\partial x\,\partial\theta}+C_1\left(\frac{\partial^2 v}{\partial x^2}+\frac{\partial^2 u}{R\,\partial x\,\partial\theta}\right)+C_2\frac{\partial^3 w}{R\,\partial x^2\partial\theta}+C_3\frac{\partial^2\varphi}{R\,\partial x\,\partial\theta}-\frac{1}{R}\left(F_1\frac{\partial^3 w}{R\,\partial x^2\partial\theta}+F_2\left(\frac{\partial^2 v}{\partial x^2}+\frac{\partial^2 u}{R\,\partial x\,\partial\theta}\right)+F_3\frac{\partial^2\varphi}{R\,\partial x\,\partial\theta}\right)-\frac{1}{R^2}\left(E_1\frac{\partial^3 w}{R^2\,\partial\theta^3}+E_2\frac{\partial^3 w}{\partial\theta\,\partial x^2}+\frac{E_3}{R}\left(\frac{\partial w}{\partial\theta}+\frac{\partial^2 v}{\partial\theta^2}\right)+E_4\frac{\partial^2 u}{\partial\theta\,\partial x}+E_5\frac{\partial^2\varphi}{\partial\theta\,\partial x}\right)=\left(\rho h+\rho' h_1\right)\frac{\partial^2 v}{\partial t^2} \tag{30}$$

$$D_1\frac{\partial^4 w}{\partial x^4}+D_2\frac{\partial^4 w}{R^2\,\partial x^2\,\partial\theta^2}+D_3\frac{\partial^3 u}{\partial x^3}+\frac{D_4}{R}\left(\frac{\partial^2 w}{\partial x^2}+\frac{\partial^3 v}{\partial x^2\,\partial\theta}\right)+D_5\frac{\partial^3\varphi}{\partial x^3}+\frac{2}{R}\left(F_1\frac{\partial^4 w}{R\,\partial x^2\,\partial\theta^2}+F_2\left(\frac{\partial^3 v}{\partial x^2\,\partial\theta}+\frac{\partial^3 u}{R\,\partial x\,\partial\theta^2}\right)+F_3\frac{\partial^3\varphi}{R\,\partial x\,\partial\theta^2}\right)+\frac{1}{R^2}\left(E_1\frac{\partial^4 w}{R^2\,\partial\theta^4}+E_2\frac{\partial^4 w}{\partial x^2\,\partial\theta^2}+\frac{E_3}{R}\left(\frac{\partial^2 w}{\partial\theta^2}+\frac{\partial^3 v}{\partial\theta^3}\right)+E_4\frac{\partial^3 u}{\partial x\,\partial\theta^2}+E_5\frac{\partial^3\varphi}{\partial x\,\partial\theta^2}\right)-\frac{1}{R}\left(\frac{B_1}{R}\left(w+\frac{\partial v}{\partial\theta}\right)+B_2\frac{\partial u}{\partial x}+B_3\frac{\partial^2 w}{R^2\,\partial\theta^2}+B_4\frac{\partial^2 w}{\partial x^2}+B_5\frac{\partial\varphi}{\partial x}\right)=\left(\rho h+\rho' h_1\right)\frac{\partial^2 w}{\partial t^2} \tag{31}$$

The electric displacements in the piezoelectric layer, on the other hand, are expressed as follows,

$$D_x=-\Xi_{33\mathrm{p}}\frac{\partial\varphi}{\partial x}+e_{33\mathrm{p}}\varepsilon_x+e_{31\mathrm{p}}\varepsilon_\theta \tag{32}$$

$$D_\theta=-\Xi_{11\mathrm{p}}\frac{\partial\varphi}{R\,\partial\theta}+e_{15}\gamma_{x\theta} \tag{33}$$

$$D_r=0 \tag{34}$$

where $\Xi_{33\mathrm{p}}=\Xi_{33}+(e_{31}^2/c_{11})$, $\Xi_{11\mathrm{p}}=\Xi_{11}+(e_{15}^2/c_{55})$, are effective dielectric coefficients in the piezoelectric layer for plane stress problem.

Satisfying the Maxwell equation $\int_{\frac{h}{2}}^{\frac{h}{2}+h_1}\nabla D\,\mathrm{d}z=0$, in view of Eqs. (32)–(34), yields,

$$-\Xi_{33\mathrm{p}}\frac{\partial^2\varphi}{\partial x^2}-\Xi_{11\mathrm{p}}\frac{\partial^2\varphi}{R^2\,\partial\theta^2}+e_{33\mathrm{p}}\frac{\partial^2 u}{\partial x^2}-\frac{e_{33\mathrm{p}}}{2}(h+h_1)\frac{\partial^3 w}{\partial x^3}+\frac{e_{31\mathrm{p}}}{R}\left(\frac{\partial w}{\partial x}+\frac{\partial^2 v}{\partial x\,\partial\theta}\right)-\frac{e_{31\mathrm{p}}}{R^2}(h+h_1)\frac{\partial^3 w}{\partial x\,\partial\theta^2}+e_{15}\left(\frac{\partial^2 v}{R\,\partial x\,\partial\theta}+\frac{\partial^2 u}{R^2\,\partial\theta^2}\right)-e_{15}(h+h_1)\frac{\partial^3 w}{R^2\,\partial x\,\partial\theta^2}=0 \tag{35}$$

3. Dispersive characteristics

The most important special case results from the axi-symmetric motion. Thus, if $(\partial/\partial\theta)=0$, Eqs. (29)–(31) and (35) become,

$$A_1\frac{\partial^2 u}{\partial x^2}+\frac{A_2}{R}\frac{\partial w}{\partial x}+A_3\frac{\partial^3 w}{\partial x^3}+A_5\frac{\partial^2\varphi}{\partial x^2}=\left(\rho h+\rho' h_1\right)\frac{\partial^2 u}{\partial t^2} \tag{36}$$

$$\left(C_1-\frac{F_2}{R}\right)\frac{\partial^2 v}{\partial x^2}=\left(\rho h+\rho' h_1\right)\frac{\partial^2 v}{\partial t^2} \tag{37}$$

$$D_1\frac{\partial^4 w}{\partial x^4}+D_3\frac{\partial^3 u}{\partial x^3}+\frac{D_4}{R}\frac{\partial^2 w}{\partial x^2}+D_5\frac{\partial^3\varphi}{\partial x^3}-\frac{1}{R}\left(\frac{B_1}{R}w+B_2\frac{\partial u}{\partial x}+B_4\frac{\partial^2 w}{\partial x^2}+B_5\frac{\partial\varphi}{\partial x}\right)=\left(\rho h+\rho' h_1\right)\frac{\partial^2 w}{\partial t^2} \tag{38}$$

$$-\Xi_{33\mathrm{p}}\frac{\partial^2\varphi}{\partial x^2}+e_{33\mathrm{p}}\frac{\partial^2 u}{\partial x^2}-\frac{e_{33\mathrm{p}}}{2}(h+h_1)\frac{\partial^3 w}{\partial x^3}+\frac{e_{13\mathrm{p}}}{R}\frac{\partial w}{\partial x}=0 \tag{39}$$

It can be observed that Eq. (37) is decoupled from the remaining equations, which can be written as,

$$\frac{\partial^2 v}{\partial x^2}=\frac{1}{c_{\mathrm{t}}^2}\frac{\partial^2 v}{\partial t^2} \tag{40}$$

where

$$c_{\mathrm{t}}=\sqrt{\frac{C_1-(F_2/R)}{\rho h+\rho' h_1}}=\sqrt{\frac{Gh+c_{44}h_1(1-((h+h_1)/R))}{\rho h+\rho' h_1}}$$

and

$$G=\frac{E}{2(1+v)}$$

This is the pure torsional motion of the shell. It can be seen clearly from the above expression that the piezoelectric layer plays a role as a composite part in the structure, as the elastic modulus $c_{44\mathrm{p}}$ is shown in the expression. The mechanical coupling effect by the piezoelectric layer is quite obvious. However, no piezoelectric effect is found, for no piezoelectric coefficients or dielectric constants are involved in the expression of the torsional phase velocity. Further, it can be seen that the solution of the torsional wave phase velocity by membrane theory (Wang, 2001) can be obtained if F_2 is set to be zero in the current study by bending theory. Thus, the difference of the results by bending theory and membrane theory is clearly observed, and this discrepancy can be evaluated from Eq. (40).

Now consider the wave propagation from the other governing equations by letting,

$$u=U\mathrm{e}^{\mathrm{i}\xi(x-ct)} \tag{41}$$

$$w=W\mathrm{e}^{\mathrm{i}\xi(x-ct)} \tag{42}$$

$$\varphi=\Phi\mathrm{e}^{\mathrm{i}\xi(x-ct)} \tag{43}$$

where ξ and c are wave number and wave phase velocity respectively; U, W, and Φ are magnitudes of variables of the wave propagation.

Substituting wave solutions from Eqs. (41)–(43) into Eq. (39) yields,

$$\Phi=\frac{e_{33\mathrm{p}}}{\Xi_{33\mathrm{p}}}U-\frac{\mathrm{i}e_{31\mathrm{p}}}{\Xi_{33\mathrm{p}}}W\left(\frac{1}{R\xi}+\frac{(h+h_1)}{2}\frac{e_{33\mathrm{p}}}{e_{31\mathrm{p}}}\xi\right) \tag{44}$$

Substituting Eq. (44) into Eq. (38) yields the relationship between W and U as follows,

$$W=\mathrm{i}\xi G_1 U \tag{45}$$

where

$$G_1 = \frac{G_2}{(\rho h + \rho' h_1)\omega^2 - G_3}, \quad G_2 = \frac{B_2}{R} + D_3\xi^2 + \frac{e_{33p}}{\Xi_{33p}}\left(\frac{B_5}{R} + D_5\xi^2\right),$$
$$G_3 = \frac{e_{31p}}{\Xi_{33p}}\left(D_5\xi^2 + \frac{B_5}{R}\right)\left(\frac{1}{R} + \frac{h+h_1}{2}\frac{e_{33p}}{e_{31p}}\xi^2\right) + \frac{B_1}{R^2} + \frac{D_4\xi^2}{R} - \frac{B_4\xi^2}{R} - D_1\xi^4$$

where $\omega = c\xi$ is circular frequency of the motion.

Introducing Eq. (45) into Eq. (44) gives,

$$\Phi = G_4 U \tag{46}$$

where

$$G_4 = \frac{e_{33p}}{\Xi_{33p}} + \frac{\xi e_{31p} G_1}{\Xi_{33p}}\left(\frac{1}{R\xi} + \frac{h+h_1}{2}\frac{e_{33p}}{e_{31p}}\xi\right)$$

Substituting Eqs. (45) and (46) into Eq. (36), we have

$$\left(-A_1\xi^2 - \frac{A_2}{R}G_1\xi^2 + A_3\xi^4 G_1 - A_5 G_4\xi^2\right)U = -\left(\rho h + \rho' h_1\right)\omega^2 U \tag{47}$$

Consider the large and small wave number limits. As $\xi \to 0$, the cut-off frequencies are:

$$\omega_1 = 0,$$

and

$$\omega_2 = \frac{1}{R}\sqrt{\left(B_1 + \frac{B_5 e_{31p}}{\Xi_{33p}}\right)\Big/(\rho h + \rho' h_1)} = \frac{1}{R}\sqrt{\left(\frac{Eh}{1-v^2} + c_{11p}h + \frac{h_1 e_{31p}^2}{\Xi_{33p}}\right)\Big/(\rho h + \rho' h_1)} \tag{48}$$

If no piezoelectric layer is surface bonded on the shell, i.e. $h_1 = 0$, we have

$$\omega_2 = \frac{1}{R}\sqrt{\frac{E}{\rho(1-v^2)}}$$

This result is exactly the same with that obtained by membrane theory (Wang, 2001).

The dispersive solution for this piezoelectric coupled membrane shell is then obtained as,

$$\left(\rho h + \rho' h_1\right)c^2 - A_1 - \frac{A_2}{R}G_1 + A_3\xi^2 G_1 - A_5 G_4 = 0 \tag{49}$$

Rewrite Eq. (49) in the expression,

$$\left(\rho h + \rho' h_1\right)^2 c^4 - H_1\left(\rho h + \rho' h_1\right)c^2 + H_2 = 0 \tag{50}$$

where

$$H_1 = A_1 + A_5\frac{e_{33p}}{\Xi_{33p}} + \frac{G_3}{\xi^2},$$
$$H_2 = -\frac{G_2 A_2}{R\xi^2} + G_2 A_3 - \frac{G_2 A_5}{\xi}\frac{e_{31p}}{\Xi_{33p}}\left(\frac{1}{R\xi} + \frac{h+h_1}{2}\frac{e_{33p}}{e_{31p}}\xi\right) + \frac{G_3}{\xi^2}\left(A_1 + A_5\frac{e_{33p}}{\Xi_{33p}}\right)$$

The solutions for Eq. (50) are obtained herein,

$$c_1^2 = \frac{1}{2(\rho h + \rho' h_1)}\left(H_1 - \sqrt{H_1^2 - 4H_2}\right) \tag{51}$$

$$c_2^2 = \frac{1}{2(\rho h + \rho' h_1)}\left(H_1 + \sqrt{H_1^2 - 4H_2}\right) \tag{52}$$

As $\xi \to 0$, the phase velocity is,

$$c_0^2 = \frac{1}{(\rho h + \rho' h_1)}\left(A_1 + A_5\frac{e_{33\mathrm{p}}}{\Xi_{33\mathrm{p}}} - \frac{B_2 + (B_5 e_{33\mathrm{p}}/\Xi_{33\mathrm{p}})}{B_1 + (B_5 e_{31\mathrm{p}}/\Xi_{33\mathrm{p}})}\left(A_2 + A_5\frac{e_{31\mathrm{p}}}{\Xi_{33\mathrm{p}}}\right)\right) \tag{53}$$

and we have the velocity at limit case, $h_1 = 0$,

$$c^2 = \frac{E}{\rho} \tag{54}$$

As $\xi \to \infty$, the phase velocity $c_{\mathrm{inf}\ 1}^2$ goes to the limit value as,

$$c_{\mathrm{inf}\ 1}^2 = \frac{1}{(\rho h + \rho' h_1)}\left(A_1 + A_5\frac{e_{33\mathrm{p}}}{\Xi_{33\mathrm{p}}} + \left(A_3 - A_5\frac{h + h_1}{2}\frac{e_{33\mathrm{p}}}{\Xi_{33\mathrm{p}}}\right)\frac{D_3 + D_5\frac{e_{33\mathrm{p}}}{\Xi_{33\mathrm{p}}}}{D_5\frac{(h+h_1)}{2}\frac{e_{33\mathrm{p}}}{\Xi_{33\mathrm{p}}} - D_1}\right) \tag{55}$$

The wave velocity of the host metal is obtained from the above equation at $h_1 = 0$,

$$c_1^2 = \frac{E}{\rho(1 - v^2)} \tag{56}$$

On the other hand, $c_{\mathrm{inf}\ 2}^2$ show a proportional variation with wave number at $\xi \to \infty$,

$$c_{\mathrm{inf}\ 2}^2 = \frac{1}{(\rho h + \rho' h_1)}\left(\frac{e_{33\mathrm{p}}}{\Xi_{33\mathrm{p}}}\frac{h + h_2}{2}D_5 - D_1\right)\xi^2 = \frac{1}{(\rho h + \rho' h_1)}K\xi^2 \tag{57}$$

This result at $h_1 = 0$ shown above is consistent with the results for pure metal cylindrical shell (Graff, 1991).

$$c = h\xi\sqrt{\frac{E}{12\rho(1 - v^2)}} \tag{58}$$

4. Numerical examples

The material properties of the host shell of aluminium and gold, and the piezoelectric layer of PZT4 are listed in Table 1 for numerical analysis. In Figs. 2–5, the solutions for the torsional wave phase velocity, the phase velocities of the coupling wave mode both at zero and infinite wave number, and the cut-off frequency are plotted. To investigate the effect by the piezoelectric layer, the non-dimensional torsional velocity $\bar{c}_{\mathrm{t}}$, phase velocity at zero wave number $\bar{c}_0$, phase velocity at infinite wave number $\bar{c}_{\mathrm{inf}}$, and the cut-off frequency $\overline{\omega}$ are defined as

$$\bar{c}_{\mathrm{t}} = c_{\mathrm{t}}\Big/\sqrt{\frac{E}{2\rho(1 + v)}},\quad \bar{c}_0 = c_0\Big/\sqrt{\frac{E}{\rho}},\quad \bar{c}_{\mathrm{inf}} = c_{\mathrm{inf}}\Big/\sqrt{\frac{E}{\rho(1 - v^2)}},\quad \text{and}\quad \overline{\omega} = R\omega\Big/\sqrt{\frac{E}{\rho(1 - v^2)}}$$

For the purpose of comparison of the solutions by the membrane and bending shell theories, the solutions by membrane shell theory (Wang, 2001) are also plotted in the Figs. 2–5.

Table 1
Material properties

	Aluminium	Gold	PZT-4
Mass density (kg/m^3)	$\rho' = 2.8 \times 10^3$	$\rho' = 1.9 \times 10^4$	$\rho = 7.5 \times 10^3$
Young modulus (N/m^2)	$E = 70 \times 10^9$	$E = 78 \times 10^{10}$	$c_{11} = 132 \times 10^9$,
Poisson ratio	0.33	0.42	$c_{33} = 115 \times 10^9$,
			$c_{12} = 71 \times 10^9$, $c_{13} = 73 \times 10^9$,
			$c_{44} = 26 \times 10^9$
e_{31} (k/m^2)			-4.1
e_{33} (k/m^2)			14.1
e_{15} (k/m^2)	–	–	10.5
Ξ_{11} (ϕ/m)	–	–	5.841×10^{-9}
Ξ_{33} (ϕ/m)	–	–	7.124×10^{-9}

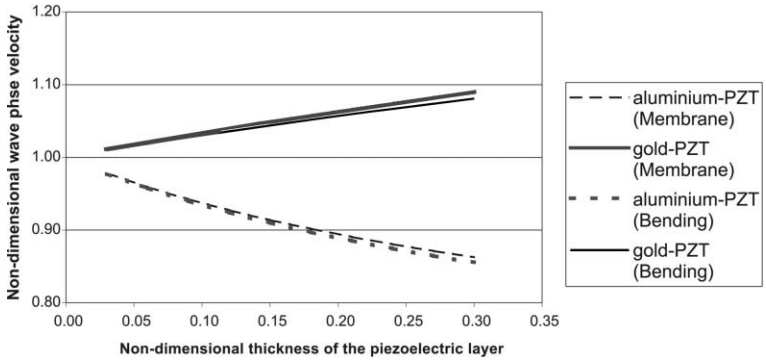

Fig. 2. Torsional wave velocity by two shell theories.

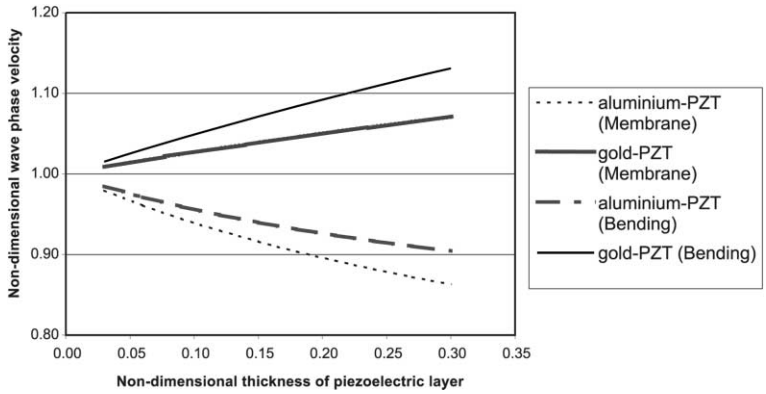

Fig. 3. Wave velocity at zero wave number by two shell theories.

In Fig. 2, the discrepancies of the torsional wave velocities by the two shell theories are shown with the change of the thickness of the piezoelectric layer. The first observation is that the velocity decreases with the increase of the thickness of the piezoelectric layer for the shell with aluminium core, and the reverse trend was found for the shell with the gold core for both membrane and bending shell theories. This observation can be expected by the fact that the piezoelectric layer is stiffer than gold core, but softer than the alu-

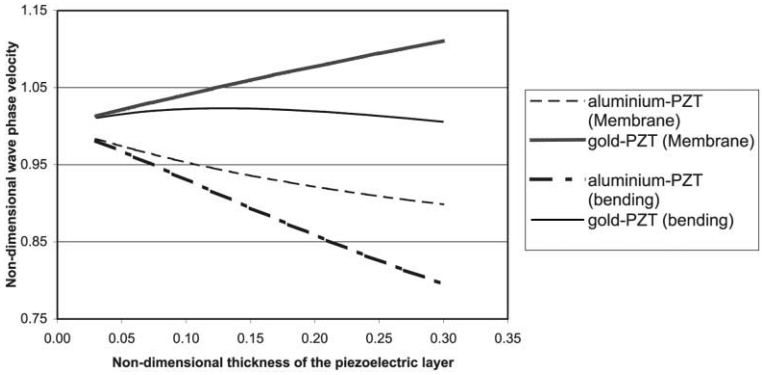

Fig. 4. Wave phase velocity at infinite wave number by two shell theories.

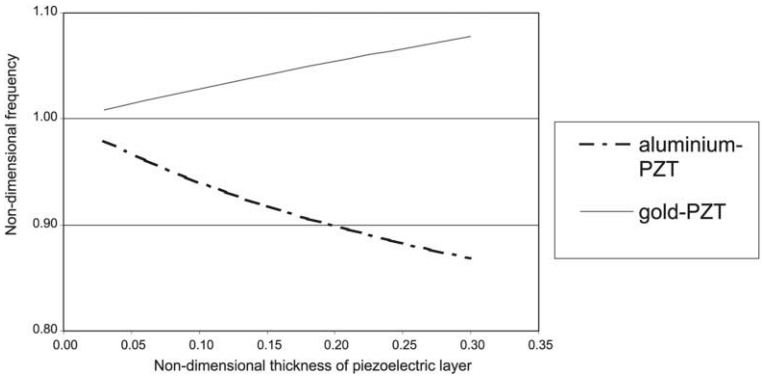

Fig. 5. Cut-off frequency by two shell theories.

minium core. The different dispersive behaviour of the gold and aluminium piezoelectric coupled cylinder is mainly due to the big differences of the Young's module of the two metals. Another observation from the figure is that the torsional wave phase velocity,

$$c_t = \sqrt{\frac{C_1 - (F_2/R)}{\rho h + \rho' h_1}} = \sqrt{\frac{Gh + c_{44}h_1(1 - ((h + h_1)/R))}{\rho h + \rho' h_1}}$$

by bending theory is lower than that obtained from membrane theory,

$$c_t = \sqrt{\frac{C_1}{\rho h + \rho' h_1}}$$

in this structure as shown in Eq. (40) since $F_2 > 0$ listed in Appendix A. This discrepancy becomes more obvious with thicker piezoelectric layer. In Figs. 3 and 4, the comparisons of wave phase velocities at zero and infinite wave number by the two shell theories are conducted separately. It is not surprised to find that, for both aluminium-PZT and gold-PZT shell structures, the wave velocities by bending theories are bigger than those by membrane theory at zero wave number, but smaller than those by membrane theory at infinite wave number. The discrepancies of the phase velocities for all the cases again become more obvious with the increase of the piezoelectric layer. Similar observations were also obtained by Greenspon (1960) when he did the comparison of the dispersion characteristics of a metallic cylindrical shell by different

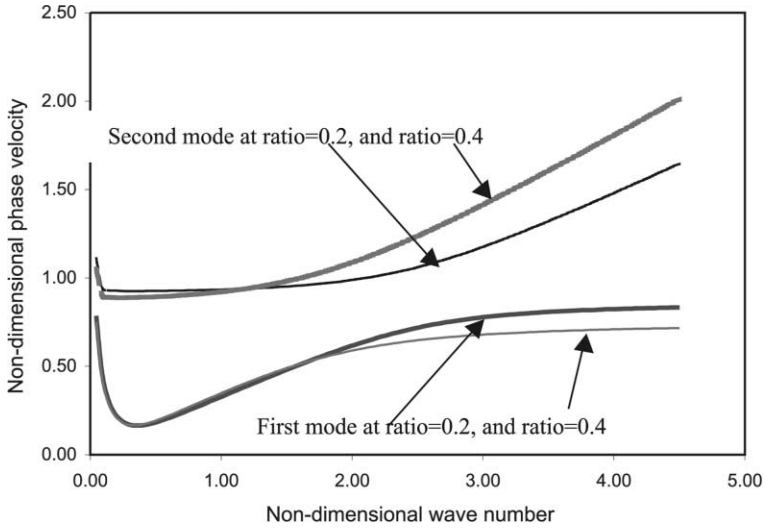

Fig. 6. Dispersion curves for aluminium-PZT shell.

approximate shell theories. One special observation from Fig. 4 shows that the variation of the phase velocity at infinite wave number for gold-PZT shell is almost independent of the thickness of the piezoelectric layer. From the discussion of the cut-off frequency of the cylindrical shell in Eq. (48), it is concluded that the result of the cut-off frequency is independent of the theories used in the model. This conclusion is observed from Eq. (48) and shown in Fig. 5, which is also derived by Wang (2001). The cut-off frequency in the aluminium-PZT shell decreases with the increase of the piezoelectric layer, however, the reverse result is shown for the gold-PZT shell.

The dispersion curves of the wave phase velocities for the first mode and the second wave mode at thickness ratios of 0.2 and 0.4 for aluminium-PZT and gold-PZT cylindrical shell separately by bending theory are shown in Figs. 6 and 7. The curves show different variation for different ratios of the piezoelectric

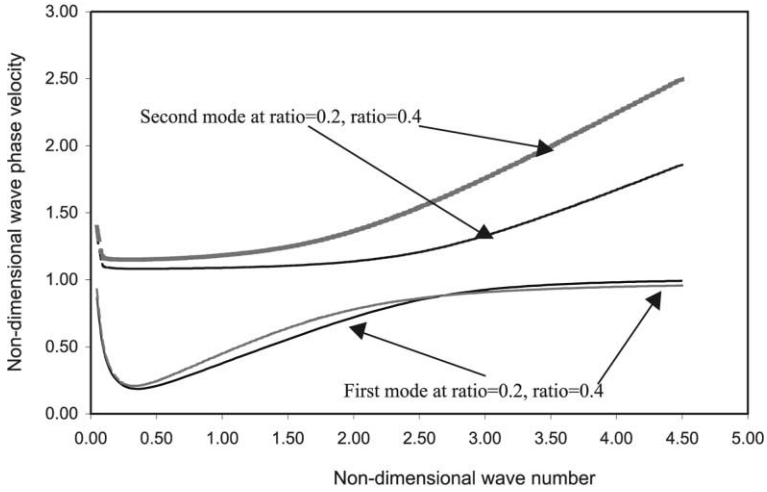

Fig. 7. Dispersion curves for gold-PZT shell.

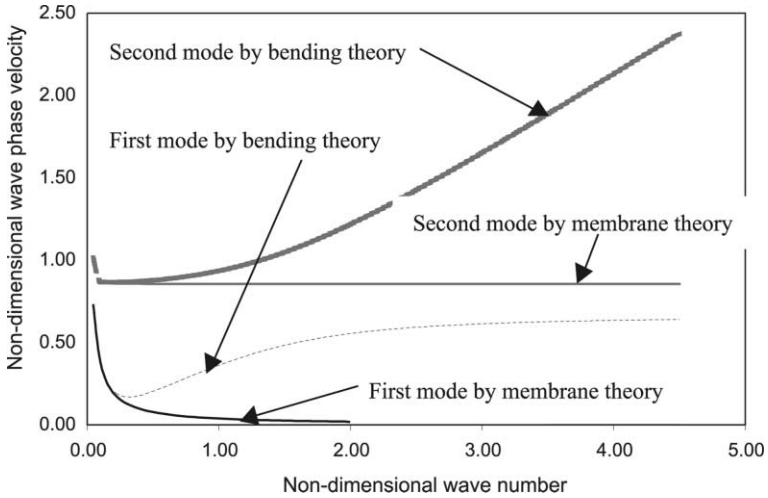

Fig. 8. Comparison of dispersion curves of aluminium-PZT shell by membrane and bending theory at ratio = 0.3.

layer at higher wave number. In addition, the phase velocity of the first mode approaches to an asymptotic value, whereas, the velocity for the second wave mode show its linear variation with the wave number. The analytical solutions for the two phase velocities are also shown in Eqs. (55) and (57).

The comparison of the dispersion curves for the piezoelectric cylindrical shell by the membrane and bending theories are illustrated in Fig. 8. As can be seen that the dispersion curves by the two theories coincide completely at the lower wave number. Nevertheless, at higher wave number, they go to different asymptotic solutions as discussed in this paper for the piezoelectric coupled shell, as well as by Greenspon (1960) in his studies of comparison of the wave propagation by different theories for a pure metallic cylindrical shell.

5. Concluding remarks

This paper studies the wave propagation in a piezoelectric coupled cylindrical shell with bending resistance. The mathematical model for the wave propagation is presented, and the axi-symmetric motion is investigated. The piezoelectric coupling effects are fully modeled in the mechanics model for this piezoelectric coupled cylindrical shell. The limit of the theory lies in the fact the piezoelectric layer must be thin enough so that the kinematics field proposed in the paper may be satisfied. The solutions for the decoupled torsional phase velocity and the coupled transverse phase velocities of the first and second wave mode are obtained theoretically. The comparison of the results by the bending theory and membrane theory is conducted in numerical simulations. The main results from simulations show that the solutions of the wave propagation in the piezoelectric cylindrical shell by bending theory and membrane theory display bigger difference with the thicker piezoelectric layer and at higher wave number. Thus, the further work will focus on the wave propagation in the piezoelectric coupled cylindrical shells by more general shell theories to account for the effects of shear and bending or rotary inertia to obtain more accurate results in the application of wave propagation of piezoelectric structures.

The results of this paper can serve as a reference for future study on wave propagation in piezoelectric coupled structures as well as in the design of smart structures incorporating piezoelectric materials.

Acknowledgements

The work in this paper is supported by the research grant from National University of Singapore, R-264-000-113-112. The author also appreciates the constructive comments from the reviewers.

Appendix A

$$A_1 = \frac{Eh}{1-v^2} + c_{33\mathrm{p}}h_1, \quad A_2 = \frac{Ehv}{1-v^2} + c_{13\mathrm{p}}h_1, \quad A_3 = -\frac{c_{33\mathrm{p}}}{2}\left(hh_1 + h_1^2\right)$$

$$A_4 = -\frac{c_{13\mathrm{p}}}{2}\left(hh_1 + h_1^2\right), \quad A_5 = e_{33\mathrm{p}}h_1$$

$$B_1 = \frac{Eh}{1-v^2} + c_{11\mathrm{p}}h_1, \quad B_2 = \frac{Ehv}{1-v^2} + c_{13\mathrm{p}}h_1, \quad B_3 = -\frac{c_{11\mathrm{p}}}{2}\left(hh_1 + h_1^2\right)$$

$$B_4 = A_4 = -\frac{c_{13\mathrm{p}}}{2}\left(hh_1 + h_1^2\right), \quad B_5 = e_{31\mathrm{p}}h_1$$

$$C_1 = \frac{Eh}{2(1+v)} + c_{44\mathrm{p}}h_1, \quad C_2 = -c_{44\mathrm{p}}\left(hh_1 + h_1^2\right), \quad C_3 = e_{15\mathrm{p}}h_1$$

$$D_1 = -\frac{Eh^3}{12(1-v^2)} - \frac{c_{33\mathrm{p}}}{3}\left(h_1^3 + \frac{3}{2}hh_1^2 + \frac{3}{4}h^2h_1\right)$$

$$D_2 = -\frac{Eh^3v}{12(1-v^2)} - \frac{c_{13\mathrm{p}}}{3}\left(h_1^3 + \frac{3}{2}hh_1^2 + \frac{3}{4}h^2h_1\right)$$

$$D_3 = \frac{c_{33\mathrm{p}}}{2}\left(hh_1 + h_1^2\right) = -A_3, \quad D_4 = \frac{c_{13\mathrm{p}}}{2}\left(hh_1 + h_1^2\right) = -A_4, \quad D_5 = \frac{e_{33\mathrm{p}}}{2}\left(hh_1 + h_1^2\right)$$

$$E_1 = -\frac{Eh^3}{12(1-v^2)} - \frac{c_{11\mathrm{p}}}{3}\left(h_1^3 + \frac{3}{2}hh_1^2 + \frac{3}{4}h^2h_1\right)$$

$$E_2 = -\frac{Eh^3v}{12(1-v^2)} - \frac{c_{13\mathrm{p}}}{3}\left(h_1^3 + \frac{3}{2}hh_1^2 + \frac{3}{4}h^2h_1\right) = D_2$$

$$E_3 = \frac{c_{11\mathrm{p}}}{2}\left(hh_1 + h_1^2\right) = -B_3, \quad E_4 = \frac{c_{13\mathrm{p}}}{2}\left(hh_1 + h_1^2\right) = D_4, \quad E_5 = \frac{e_{31\mathrm{p}}}{2}\left(hh_1 + h_1^2\right)$$

$$F_1 = -\frac{Eh^3}{24(1+v)} - \frac{2c_{44\mathrm{p}}}{3}\left(h_1^3 + \frac{3}{2}hh_1^2 + \frac{3}{4}h^2h_1\right), \quad F_2 = c_{44\mathrm{p}}\left(hh_1 + h_1^2\right)$$

$$F_3 = \frac{e_{15\mathrm{p}}}{2}\left(hh_1 + h_1^2\right)$$

References

Auld, B.A., 1973a. In: Acoustic Fields and Waves in Solids, vol. I. John Wiley & Sons Inc.

Auld, B.A., 1973b. In: Acoustic Fields and Waves in Solids, vol. II. John Wiley & Sons Inc.

Badcock, R.A., Birt, E.A., 2000. The use of 0–3 piezocomposite embedded Lamb wave sensors for detection of damage in advanced fibre composites. Smart Materials and Structures 9, 291–297.

Bluestein, J.L., 1969. Some simple modes of wave propagation in an infinite piezoelectric plates. Journal of the Acoustical Society of America 45, 614–620.

Campbell, C.K., 1998. Surface acoustic wave devices for mobile and wireless communications, New York: Academic.

Cooper, R.M., Naghdi, P.M., 1957. Propagation of nonaxially symmetric waves in elastic cylindrical shells. Journal of the Acoustical Society of America 29, 1365–1372.

Curtis, R.G., Redwood, M., 1973. Transverse surface waves in piezoelectric materials carrying a metal layer of finite thickness. Journal of Applied Physics 44, 2002–2007.

Ding, H.J., Chen, W.Q., Guo, Y.M., Yang, Q.D., 1997. Free vibrations of piezoelectric cylindrical shells filled with compressive fluid. International Journal of Solids and Structures 34, 2025–2034.

Donnel, L.H., 1933. Stability of Thin Walled Tubes under Torsion. NACA Rep. No. 479.

Flüggey, W., 1934. Satik und Dynamik der Schalen. Springer-Verlag, Berlin.

Graff, K.F., 1991. In: Wave Motion in Elastic Solids. Dover Publications Inc., New York.

Greenspon, J.E., 1960. Vibrations of a thick-walled cylindrical shell-comparison of the exact theory with approximate theories. Journal of the Acoustical Society of America 32, 571–578.

Lin, T.C., Morgan, G.W., 1956. A study of axisymmetric vibrations of cylindrical shells as affected by rotary inertia and transverse shear. Journal of Applied Mechanics 23, 255–261.

Love, A.E.H., 1944. A Treatise on the Mathematical Theory of Elasticity. Dover Publications Inc., New York.

Mersky, I., Herrmann, G., 1958. Axially Symmetric Motions of Thick Cylindrical Shells. Journal of Applied Mechanics 25, 97–102.

Minagawa, S., 1995. Propagation of harmonic waves in a layered elasto-piezoelectric composite. Mechanics of Materials 19, 165–170.

Mindlin, R.D., 1952. Forced thickness-shear and flexural vibrations of piezoelectric crystal plates. Journal of Applied Physics 23, 83–88.

Monkhouse, R.S.C., Wilcox, P.W., Dalton, R.P., Cawley, P., 2000. The rapid monitoring of structures using interdigital Lamb wave transducers. Smart Materials and Structures 9, 304–309.

Morgan, D.P., 1998. History of SAW devices. IEEE Int. Frequency Control Symp., 439–460.

Parton, V.Z., Kudryavtser, B.A., 1988. Electromagnetoelasticity. Gordon & Breach Science Publishers, New York.

Sanders, J.L., 1959. An improved first approximation theory for thin shells. NASA Technical Report R24.

Sun, C.T., Cheng, N.C., 1974. Piezoelectric waves on a layered cylinder. Journal of Applied Physics 45, 4288–4294.

Tiersten, H.F., 1963. Wave propagation in an infinite piezoelectric plate. Journal of the Acoustical Society of America 35, 234–239.

Varadan, V.K., Varadan, V.V., 2000. Microsensors, microelectromechanical systems (MEMS), and electronics for smart systems. Smart materials and structures 9, 953–972.

Viktorov, I.A., 1967. Rayleigh and Lamb Waves. Plenum, New York.

Viktorov, I.A., 1981. Surface Waves in Solids. Nauka, Moscow, in Russian.

Vlasov, V.Z., 1949. General Theory of Shells and its Application to Engineering. Leninggrad, Moscow.

Wang, Q., 2001. Wave propagation in a piezoelectric coupled cylindrical membrane shell. International Journal of Solids and Structures 38, 8207–8218.

White, R.M., 1998. Acoustic sensors for physical, chemical, and biochemical applications. IEEE Int. Frequency Control Symp., 587–594.